Benzoyl Transfer Reactivities of Racemic 2,4-Di-*O*-acyl-*myo*-inosityl 1,3,5-Orthoesters in the Solid State: Molecular Packing and Intermolecular Interactions Correlate with the Ease of the Reaction

Manash P. Sarmah,[a] Rajesh G. Gonnade,[b] Mysore S. Shashidhar,*[a] and Mohan M. Bhadbhade*[b]

Abstract: Racemic 2,4-di-*O*-acyl-*myo*-inosityl 1,3,5-orthoesters undergo transesterification catalyzed by sodium carbonate with varying ease of reaction in the solid state; reactions in solution and melt do not show such varied differences. An interesting crystal of a 1:1 molecular complex of highly reactive racemic 2,4-di-*O*-benzoyl-*myo*-inosityl 1,3,5-orthoformate and its orthoacetate analogue exhibited better reactivity than the latter component alone. Single-crystal X-ray structures of the reactants have been correlated with the observed differences in the acyl-transfer efficiencies in the solid state. Although each of the derivatives helically self-assembles around the crystallographic 2_1 axis linked through O−H···O hydrogen bonding, the pre-organization of the reactive groups (C=O [El] and OH [Nu]), C−H···O and the C−H···π interactions are significantly more favourable for the reactive derivatives than the less reactive ones. Bond-length distributions also showed differences; the O−C bond of the axial benzoyl group, which gets cleaved during the reaction, is longer (1.345–1.361 Å) relative to the chemically equivalent O−C bond of the equatorial benzoyl group (1.316–1.344 Å) in the reactive derivatives. These bond-length differences are not significant in the less reactive derivatives. The overall molecular organization is different too; the strikingly discrete helices, which may be viewed as "reaction tunnels" and are held by interhelical interactions, are clearly evident in the reactive derivatives in comparison with the less reactive ones.

Keywords: hydrogen bonds · inositol · solid-state reactions · structure elucidation · transesterification

Introduction

Acyl-transfer reactions, ubiquitous in natural systems,[1] have been extensively studied in the solution state;[2] the only report on acyl-transfer reactions in the solid state was from this laboratory.[3] Solid-state organic reactions,[4] offering a potential for carrying out solvent-free reactions, are attractive from a synthetic as well as a mechanistic point of view. Single-crystal to single-crystal chemical transformations provide valuable information on the mechanism of reactions, but relatively few examples of such reactions are known in the literature.[5] In most solid-state reactions, the crystal lattice of the reactants collapses with the onset of the reaction. However, a reactant crystal structure alone can provide valuable information on the mechanism of a reaction.[6] Earlier, we reported a very facile transesterification reaction of **1** (Scheme 1) in the crystalline state;[7] the reaction efficiency was correlated with the juxtaposition of the reactants in crystals.[3,6] The structure of **1** showed helical self-assembly[8] formed through O−H···O hydrogen bonding, which prompted us to investigate the solid-state acyl-transfer reactivities of a few more hydroxyl ester derivatives based on *myo*-inosityl 1,3,5-orthoesters to assess the influence of the "pre-organization" factor of reactants in crystals on the solid-state intermolecular acyl-transfer reactivity. In this paper, we have correlated the acyl-transfer efficiencies of diesters **1–3** with the molecular packing and intermolecular interactions

[a] M. P. Sarmah, Dr. M. S. Shashidhar
Division of Organic Synthesis
National Chemical Laboratory
Pune 411 008 (India)
Fax: (+91) 20-589-3153
E-mail: shashi@dalton.ncl.res.in

[b] R. G. Gonnade, Dr. M. M. Bhadbhade
Center for Materials Characterization
National Chemical Laboratory
Pune 411 008 (India)
Fax: (+91) 20-258-93044
E-mail: mohanb@sil.ncl.res.in

Supporting Information for this article is available on the WWW under http://www.chemeurj.org/ or from the author.

 DOI: 10.1002/chem.200400851

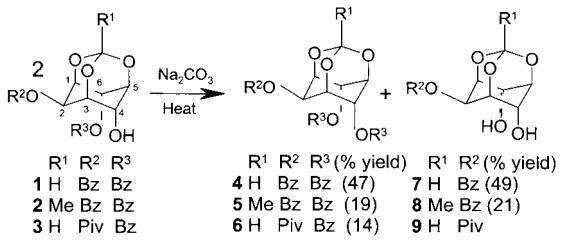

Scheme 1. Structures of *myo*-inosityl orthoester derivatives **1**–**3** and their transesterification reactions in the crystalline state.

that exist in their crystals. Our studies strongly suggest that both the "right" orientation of the neighboring reacting molecules and intermolecular interactions that maintain the topochemical control are important[9] in determining the ease and specificity of the reaction. A co-crystal of **1** and **2** (hereafter **1·2**), which exhibited better reactivity than its component **2**, reinforces the importance of intermolecular interactions present in crystals.

Results and Discussion

The structures of *myo*-inosityl orthoester derivatives investigated for solid-state reactivity in the present study are shown in Scheme 1. The racemic diester **2** was prepared by the dibenzoylation of *myo*-insoityl 1,3,5-orthoacetate, while racemic **3** was prepared by the sequential acylation of *myo*-insoityl 1,3,5-orthoformate with pivaloyl chloride followed by benzoyl chloride. The details of synthesis and characterization are described in the Experimental Section.

Since the crystal structures (described later) of **1**, **2**, and **3** showed similar molecular organization, we attempted co-crystallizations of various combinations, such as **1** with **2**, **1** with **3**, and **2** with **3** and also a ternary complex of **1**, **2**, and **3** together in various stoichiometries. Of all the trials, we were fortunate to obtain crystals of the "molecular hybrid" **1·2** by co-crystallization. Interestingly, crystals of **1·2** always had a 1:1 composition of **1** and **2**, although the solution from which it was crystallized contained **1** and **2** in different ratios (in different trials).

Transesterification of *myo*-inosityl 1,3,5-orthoester derivatives: The transesterification in solid state was carried out by heating the crystals of each of the diesters (**2**, **3**, and **1·2**) with solid sodium carbonate as per the procedure reported earlier.[3] Unlike crystals of **1**, the diesters **2** and **3** produced lower yields of the transesterified products (Scheme 1) even after allowing for longer reaction times (168 h). Furthermore, the reactions resulted in the formation of several other products and were not as clean as observed for **1**.[3] In contrast to **2** and **3**, the transesterification reaction of the dibenzoates **1** and **2** in the hybrid crystals of **1·2** proceeded smoothly to afford the corresponding tribenzoates **4** and **5** (total isolated yield 41%, **4**:**5** = 67:33, by ^{1}H NMR spectroscopy) and the diols **7** and **8** (35%, **7**:**8** = 35:65) as major products in good yields, but in differing ratios.

All the reactions in the solid state were carried out at temperatures well below the melting point of the reactants to ensure that the reactions took place in the crystalline state only and not in their molten forms. However, to rule out any possibility of liquid phases being involved below the melting points of the reactants and products in these multi-component reaction mixtures, we examined the reactivities of diesters at comparable temperatures. For instance, at 100 °C, the dibenzoate **1** underwent clean reaction, while **2** and **1·2** were unreactive. At 110 °C and above, crystals of **2** and **1·2** began to react (although slowly) to give the transesterified products. At still higher temperatures, compound **2** gave a mixture of products as described earlier. None of the diesters underwent any reaction in the molten state (~180 °C) in the absence of sodium carbonate. Reactions of **1**–**3** and **1·2** in a melt with sodium carbonate afforded a mixture of products resulting from the transesterification not only from the C6-axial ester but also from C2-equatorial ester. These results exclude the possibility of formation of any molten phases during the reaction of crystals below their melting points; such an occurrence would have resulted in a loss of specificity of the transesterification reaction (under the conditions shown in Scheme 1).

The diesters **1**–**3** and the hybrid **1·2** underwent transesterification in solution as expected,[3] to afford the corresponding triesters and diols (Scheme 1). Yields for the reactions of **1**, **2**, and **3** in acetonitrile in the presence of triethylamine (144 h) were: **4** 32%, **7** 31%, **5** 30%, **8** 29%, **6** 23%, and **9** 25%. Transesterification of hybrid crystals **1·2** also proceeded smoothly in solution to yield a mixture of triesters **4** and **5** (32%, **4**:**5** = 55:45) as well as diols **7** and **8** (28%, **7**:**8** = 56:44). The acyl-transfer reaction (Scheme 1) involves the specific transfer of the C6-O-benzoyl group (electrophile, El = C=O) of one molecule of the diester to the C4-hydroxyl group (nucleophile, Nu = OH) of another in the crystalline state as well as in solution. We have shown[10] that this specific transesterification reaction in solution is due to the intramolecular catalysis of the C4-axial hydroxyl group for the transfer of the C6-O-benzoyl group. Comparable yields in solution in contrast to the significant variations in the solid state reactivities of **1**–**3** and **1·2** can be attributed to the differences in the molecular packing in crystals.

Crystal-structure analyses of the diesters **1**–**3** and **1·2** were carried out to gain further insight of the differences in their solid-state reactivities. Thermal analysis of the inositol derivatives showed that the crystals did not undergo any phase transition upon heating. As was seen for **1** by X-ray powder diffraction, the mixing and grinding of the diesters **2**, **3**, and **1·2** with sodium carbonate did not result in a new crystalline phase.[3] The crystal structure of **1** re-determined at higher temperature (60 °C) did not show any significant increase of the anisotropies of the reactive functional groups (benzoyl and hydroxyl).

Structures of 2, 3, and 1·2: The relevant crystallographic data for the diesters **2**, **3**, and **1·2** are recorded in Table 1. All the structures belong to monoclinic space groups with a

Table 1. Summary of crystal data, data collection, structure solution, and refinement details.

	2	**3**	**1·2**
formula	$C_{22}H_{20}O_8$	$C_{19}H_{22}O_8$	$C_{43}H_{38}O_{16}$
M_r	412.38	378.37	810.73,
crystal size [mm]	$0.75\times0.50\times0.17$	$0.51\times0.50\times0.49$	$0.58\times0.24\times0.18$
T [K]	293(2)	293(2)	293(2)
crystal system	monoclinic	monoclinic	monoclinic
space group	$P2_1/n$	$P2_1/n$	Cc
a [Å]	13.592(6)	11.4581(13)	27.291(9)
b [Å]	9.677(4)	10.1522(11)	9.483(3)
c [Å]	15.298(6)	16.7158(18)	16.880(5)
β [°]	97.762(7)	104.731(2)	116.944(5)
V [Å^3]	1993.7(14)	1880.5(4)	3894(2)
Z	4	4	4
$F(000)$	864	800	1696
ρ_{calcd} [g cm^{-3}]	1.374	1.336	1.383
μ [mm^{-1}]	0.105	0.105	0.107
absorption correction	multiscan	multiscan	multiscan
max/min transmission	0.9820/0.9250	0.9502/0.9481	0.9807/0.9407
reflns collected	9736	11323	17787
unique reflns	3513	3292	6835
observed reflns	2710	2892	5290
index range	$-10\le h\le16$, $-11\le k\le11$, $-18\le l\le18$	$-13\le h\le13$, $-11\le k\le12$, $-19\le l\le19$	$-32\le h\le32$, $-11\le k\le11$, $20\le l\le20$
R_1 [$I>2\sigma(I)$]	0.0457	0.0522	0.0506
wR_2	0.1229	0.1416	0.1191
goodness-of-fit	1.046	1.057	1.059
$\Delta\rho_{max/min}$ [e Å^{-3}]	−0.166/0.175	−0.235/0.312	−0.180/0.357

strikingly similar unique b axis (~10 Å, Figure 1). In crystals of **1–3**, the molecules assemble to form a helix around the crystallographic twofold screw axis (Figure 1A, B, and C), while in crystals of **1·2** such a molecular association is around a noncrystallographic axis (Figure 1D). The successive molecules along the helix are linked by O−H···O hydrogen bonding; the OH group at the C4 position donates its H atom to the carbonyl oxygen O7 of the C2-O-acyl group. It is worth noting that O···O distances (Table 2) are somewhat longer in the reactive crystals of **1** and **1·2** (ranging from 2.816(5)–2.871(7) Å) with respect to the less reactive compounds **2** and **3** (2.775(2)–2.782(2) Å); angles D−H···A do not show any marked differences. The carbonyl oxygen atom O8 of the reactive C6-O-benzoyl group does not take part in any O−H···O hydrogen bonding. The helical assembly across the twofold axis through O−H···O bonding[8] appears to be a consistent feature in the organization of these molecules. The asymmetric unit of **1·2** consists of one molecule each of **1** and **2**, which repeats along the b axis to create a pseudo-twofold screw axis, therefore the crystal space group is pseudo $C2/c$. The space group $C2/c$ embodies a twofold axis and a twofold screw axis alternating

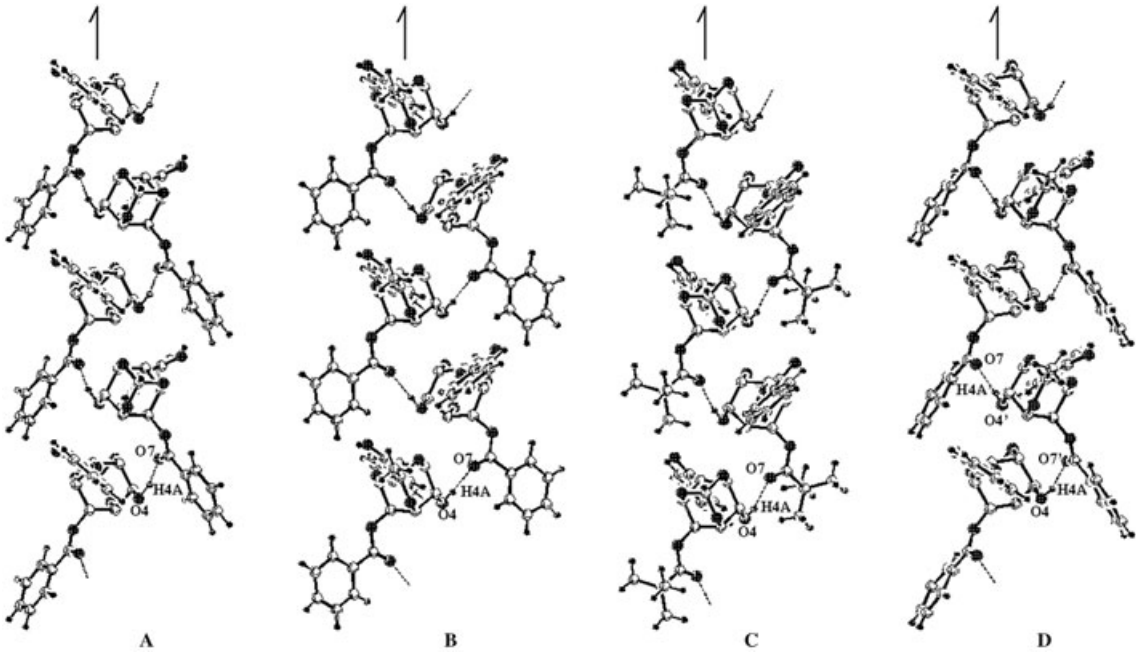

Figure 1. Helical self-assembly through O−H···O hydrogen bonding in crystals of **1** (A), **2** (B), **3** (C), and **1·2** (D) along the 2_1 axis with a similar pitch value.

Table 2. Hydrogen-bonding parameters.[a] Atom numbers refer to Figure 1.

	D–H···A	H···A [Å]	D···A [Å]	D–H···A [°]
1	O4–H4A···O7[b]	1.94	2.871(7)	158
	O4′–H4A′···O7′[c]	1.91	2.853(7)	166
2	O4–H4A···O7[d]	1.93	2.775(2)	175
3	O4–H4A···O7[e]	1.98	2.782(2)	165
1·2	O4–H4A···O7′[f]	2.06	2.848(5)	161
	O4′–H4A′···O7[g]	2.00	2.816(5)	172

[a] Values for **1** from reference [3]. [b] $1-x$, $-0.5+y$, $0.5-z$. [c] $2-x$, $0.5+y$, $0.5-z$ for the second independent molecule. [d] $1.5-x$, $-0.5+y$, $0.5-z$. [e] $1.5-x$, $-0.5+y$, $0.5-z$. [f] x, y, z. [g] x, $1+y$, z.

along the *a* axis. As the two-fold screw axis is not a true symmetry element in crystals of the **1·2** complex, the crystals belong to the space group *Cc*.

Acyl-transfer reactivities and intermolecular interactions: The helical self-assemblies in all the crystals place the reactive C6-O-benzoyl group (El) and the C4-hydroxyl group (Nu) along the helix in varying degrees of "pre-organized" geometry (Figure 2 and Table 3).[11] The El···Nu geometries are quite comparable in **1**, **2**, and **1·2**, showing favorable El···Nu interactions. In **1·2** there are two types of El···Nu interactions; one between the C6-O-benzoyl group of **1** and the C4′-hydroxyl group of **2** (benzoyl transfer at **I**) and the other between the C6′-O-benzoyl group of **2** and the C4-hydroxyl group of **1** (benzoyl transfer at **II**). However, El···Nu geometry in **3** deviates from these; the distance is somewhat longer (3.533 Å) and the angle O4···C13–O8 is 70.2° (much less than that found in reactive crystals of **1**). The low reaction efficiency of **3** relative to **1** and **1·2** can perhaps be rationalized on the basis of El···Nu geometry, but the lower reactivity of **2** cannot (Table 3). The explanation for this was sought in terms of other interactions made by the reactive groups in the crystal lattice (see below). El···Nu interactions have earlier been observed in crystals of simple organic compounds[3,12] as well as in macromolecules.[13]

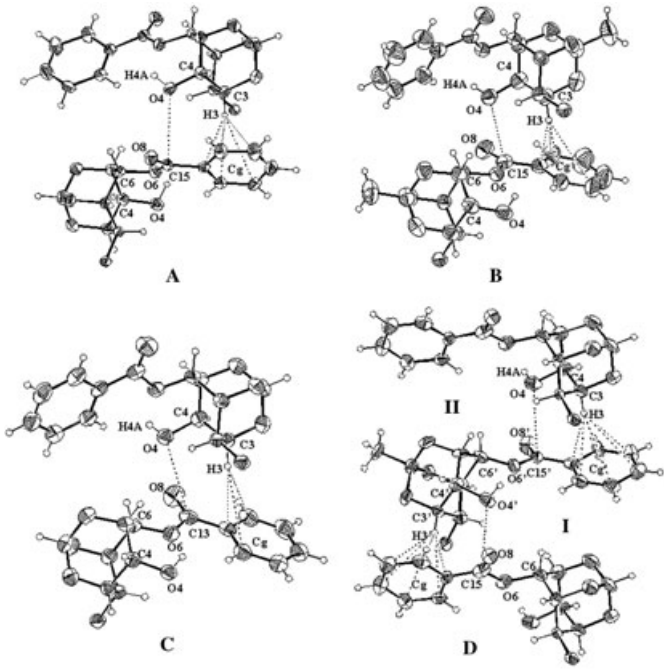

Figure 2. Relative orientation of the reacting molecules in crystals of **1** (A), **2** (B), **3** (C), and **1·2** (D) showing El···Nu and C–H···π interactions. The 2-*O*-acyl group is omitted for clarity.

Table 3. Geometry of the reacting groups. Atom numbers refer to Figure 2 [distances in Å, angles in °].

	1	**2**	**3**	**1·2**
C15(C13)···O4	3.226[a]	3.299[c]	3.533[c]	3.170[d]
	3.249[b]			3.155[e]
∢O4···C15(C13)–O8	88.1[a]	84.01[c]	70.21[c]	85.9[d]
	89.9[b]			88.4[e]
∢C4–O4···C15(C13)	117.6[a]	97.20[c]	97.65[c]	117.6[d]
	113.1[b]			116.1[e]
∢H4A–O4···C15(C13)	113.1[a]	105.8[c]	112.68[c]	107.9[d]
	110.0[b]			119.8[e]

[a] $1-x$, $-0.5+y$, $0.5-z$. [b] $2-x$, $0.5+y$, $0.5-z$ for the second independent molecule [c] $1.5-x$, $-0.5+y$, $0.5-z$. [d] x, y, z. Benzoyl transfer at **I** **1**→**2**. [e] x, $1+y$, z. Benzoyl transfer at **II** **2**→**1**.

Although the gross organization of the molecules in crystals of **1–3** and **1·2** is similar, significant differences are noticeable in the O–C bond lengths, and C–H···π[14] and C–H···O[15] contacts (see the Supporting Information for geometrical parameters). The O–C bond-length distribution shows a significant trend in accordance with acyl-transfer reactivities. The O6–C15 bond of the axial benzoyl group, which gets cleaved during the reaction, is consistently longer (1.345–1.361 Å) in the reactive crystals of **1** and **1·2** than the chemically equivalent O2–C8 bond (1.316–1.344 Å) of the equatorial benzoyl group. The difference in the corresponding axial and equatorial O–C bond lengths in **2** and **3** is not very significant. The lengthening of the O–C bond in **1** and **1·2** could be due to stronger El···Nu interactions. The geometry of C–H···π contacts made by the C3–H3 of the inositol ring with the phenyl ring of the C6-O-benzoyl group from the next molecule along the helix in **1** and **1·2** is significantly better than in **2** and **3**. It is interesting to note a significant improvement in these contacts in the molecular complex **1·2** (Figure 2D) with respect to the crystals of **2** alone. In crystals of **1–3** and **1·2** the carbonyl oxygen atom O8 of the axial benzoate makes short contacts with C1–H1. Additionally in crystals of **1**, the C6-O-benzoyl group of one of the molecules in the asymmetric unit makes two C–H···O contacts along the helix, while in **1·2** such a short contact is somewhat compromised on the angles along the helix. Another notable feature that separates reactive crystals from the less reactive ones is the packing of the helices. Helices in **1** and **1·2** are packed much more discretely than those in **2** and **3** providing a well-guided "reaction tunnel" throughout the crystal (Figure 3).

The results presented so far and the foregoing discussion can be summarized as follows. The structure correlation,[11] and computational[16] and experimental studies[3] in the crystalline state suggest that the "pre-organization" of the El (C=O) and Nu (OH) groups close to the tetrahedral angle

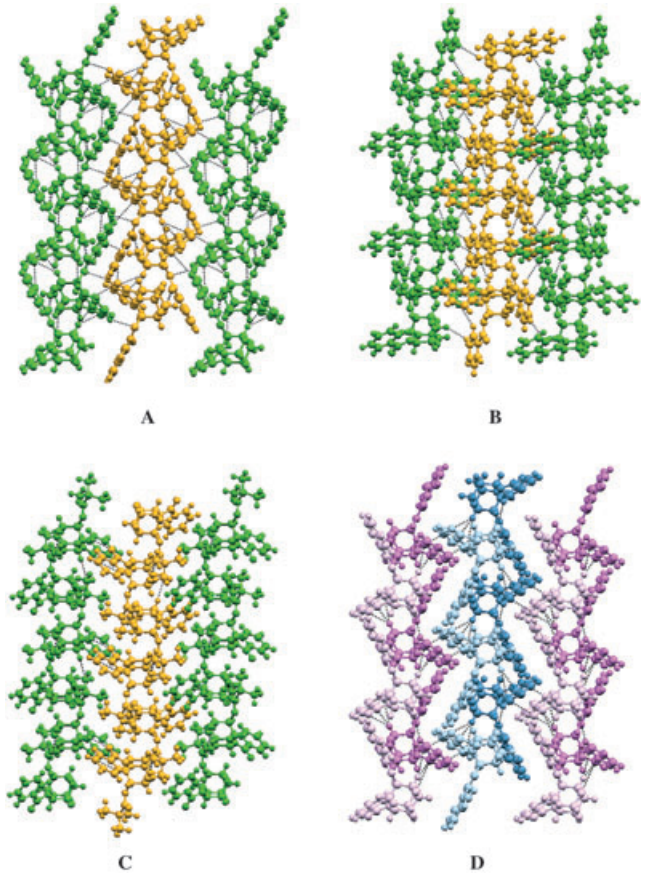

Figure 3. Packing of helices in crystals of **1** (A), **2** (B), **3** (C), and **1·2** (D). Discrete helices are seen in reactive crystals of **1** (A) and **1·2** (D), whereas such well-defined channels are not noticeable in less reactive **2** (B) and **3** (C). The colour scheme is used to distinguish the neighboring helices in A, B, and C; molecules of **1** (light pink or light blue) and **2** (dark pink or dark blue) make a single hybrid helix seen in D. Dotted lines in all the figures indicate C–H···O or C–H···π contacts.

(Nu···C=O ~110°) is an essential pre-requisite for the addition of the Nu to a carbonyl group. A comparison of the structures of **1**–**3** and **1·2** show (Figure 1A, B, C, and D) that self-assembly around the twofold axis in **2**, **3**, and **1·2** results in moderate to excellent (as observed in crystals of **1**) juxtaposition of the reactive groups. However, the favorable geometry of the reactants alone does not completely explain the facility of the transesterification reaction (Scheme 1). The reaction efficiencies can be explained if the variation in O–C bond lengths and the geometry of weak interactions[14,15] that the reactive benzoyl group makes with the neighboring molecules are taken into account. The clean reactions in **1** and **1·2** and not so clean reactions, with the emergence of other side products, in **2** and **3** imply the involvement of weak intermolecular interactions during the reaction in crystals, and the facile reaction in hybrid crystals of **1·2** (as above) supports this line of thought. The significance of weak intermolecular interactions is recognized in solid-state topochemical polymerization, in solid-to-solid transformations,[6c,9] and they have also been suggested to play a significant role in the stability of peptides,[17] proteins,[18] and in the conformation of small organic molecules.[14a,19] However, further examples and calculations are necessary to establish the effect of weak interactions on the efficiency of the reactions in crystals discussed here.

Proposed reaction mechanism in crystals: Usually chemical reactions in crystals lead to the distortion of the crystal lattice due to the appearance of products, the only exceptions to this being single-crystal to single-crystal transformations.[5] These distortions in the starting material are usually large enough to cause a collapse of the original crystal lattice, which results in rather low conversion to the product due to loss of topochemical control. However, if the reaction proceeds in a domino fashion along an axis in the crystal of the reactant, higher conversion and better yield of the products can be expected. The examples of **1** and **1·2**, which easily undergo the heterogeneous transesterification reaction that proceeds to greater than 90% completion (revealed by the absence of the starting material), can be categorized in the above class with the reaction proceeding along the helix (Figure 3). A schematic representation of the progress of the reaction along the helix in crystals of **1** and **1·2** is shown in Scheme 2. It is very likely that the base

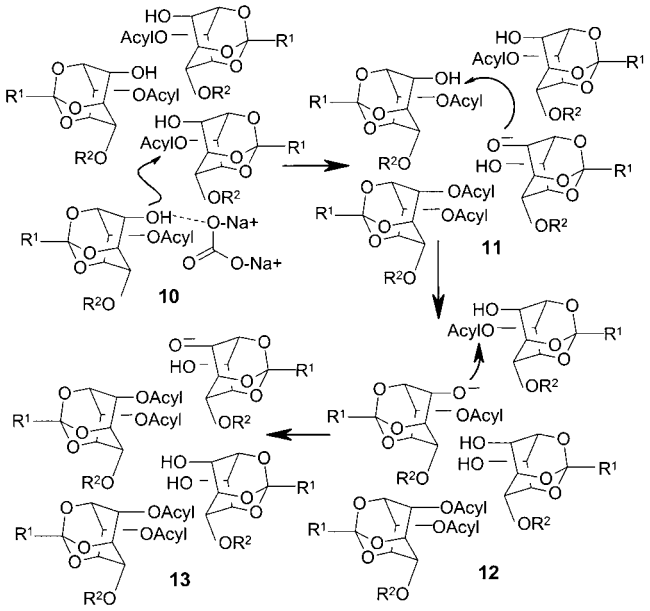

Scheme 2. The reaction along the helix in crystals of **1** and **1·2**.

(Na_2CO_3) initiates the reaction at one end of the helix by aiding the deprotonation of the C4-hydroxyl group, which enables the oxygen to attack the C6-O-benzoyl carbonyl group of the neighboring diester molecule along the helix (**10**, Scheme 2). Acyl-group transfer along the helix then generates a molecule of the triester and the corresponding diol-oxyanion (**11**). The latter functions as a base and deprotonates the hydroxyl group of its neighboring diester within the helix (**12**). The oxyanion of the dibenzoate so generated functions as a nucleophile for the attack on the

C4-O-benzoyl carbonyl group of the next molecule to generate another molecule of the tribenzoate and the diol anion (**13**). Thus in a domino fashion, these two steps lead to the generation of the two transesterification products resulting in the destruction of the helix (and eventually of the crystal) as the reaction proceeds. As mentioned above, the relative ease of reaction and yield of products correlate well with the intra- and interhelical interactions, the latter hold these helices tightly in crystals of **1** and **1·2**. In the absence of these organizations, the progress of the reaction along the helix is not likely to proceed in a domino fashion and the group transfer could terminate prematurely, lowering the yield and facility of transesterification (as in the case of **2** and **3**). The formation of other products and incomplete consumption of the starting diester as observed for the reaction of **2** and **3** can thus be rationalized.

Conclusion

We have reported a systematic investigation of the transesterification reaction of *myo*-inositol orthoformate derivatives in their crystals and correlated the reaction efficiencies with the intermolecular interactions. This reaction belongs to the class of group-transfer reactions in crystals that are rarely encountered. The fact that the less reactive **2** could be co-crystallized[14d,20] with the more reactive **1**, producing an overall reactive lattice opens up avenues for enhancing solid-state reactivities by molecular complexation.[4b] Considering the tendency of *myo*-inosityl 1,3,5-orthoester derivatives to self-assemble through O−H···O hydrogen bonds to form helices, crystal engineering studies by varying other groups on inosityl orthoesters with the aim of having a control on the regio- and/or stereospecificities of the products are underway.

Experimental Section

General methods: All the asymmetrically substituted *myo*-inositol derivatives mentioned in this paper are racemic. *myo*-Inositol 1,3,5-orthoformate,[21] *myo*-inositol 1,3,5-orthoacetate[21], and 2-*O*-pivaloyl-*myo*-inositol 1,3,5-orthoformate[22] were prepared as reported earlier. Compounds previously reported in the literature were characterized by comparison of their melting points and ^{1}H NMR spectra with those of authentic samples.

Racemic 2,4-di-*O*-benzoyl-*myo*-inositol 1,3,5-orthoacetate (2): *myo*-Inositol (5.400 g, 30.00 mmol) was allowed to react with triethyl orthoacetate (7.342 g, 45.26 mmol) in the presence of *p*-toluenesulfonic acid (0.500 g, 2.91 mmol) at 100 °C in dry DMF (50 mL) for 4 h. The reaction mixture was then cooled to room temperature, triethylamine (2 mL) was added, and the solvents were evaporated under reduced pressure to obtain a gum. The gum obtained was dissolved in dry pyridine (15 mL) and cooled in an ice bath. Benzoyl chloride (9.083 g, 64.65 mmol) was added and the solution was stirred at room temperature for 12 h. The reaction mixture was diluted with chloroform (after the evaporation of pyridine), and washed with water, saturated sodium bicarbonate solution, and brine. The chloroform extract was then dried over anhydrous sodium sulfate and chloroform was removed under reduced pressure to obtain a gum. The products were isolated by flash chromatography to obtain **2** (7.590 g, 61 %) and **5** (3.54 g, 22 %). Data for **2**: M.p. 164–165 °C; ^{1}H NMR (500 MHz, $CDCl_3$,25 °C, TMS): $\delta = 1.56$ (s, 3H), 2.60–2.61 (d, J(H,H) = 5.1 Hz, 1H; D_2O exchangeable), 4.47–4.50 (m, 1H), 4.53–4.57 (m, 1H), 4.58–4.62 (m, 1H), 4.66–4.70 (m, 1H), 5.60–5.62 (t, J(H,H) = 1.6 Hz, 1H), 5.77–5.81 (m, 1H), 7.43–7.49 (m, 4H), 7.56–7.62 (m, 2H), 8.03–8.06 (m, 2H), 8.13–8.16 ppm (m, 2H); ^{13}C NMR (50.3 MHz, $CDCl_3$, 25 °C): $\delta = 24.1$, 63.0, 67.2, 68.7, 70.4, 72.4, 108.9, 128.4, 128.5, 129.1, 129.9, 133.5, 165.3, 166.3 ppm; IR (Nujol): $\nu = 1703$ (C=O), 1724 (C=O), 3469 cm^{-1} (OH); elemental analysis calcd (%) for $C_{22}H_{20}O_8$ (412.40): C 64.08, H 4.89; found: C 63.70, H 4.99.

Racemic 2-*O*-pivaloyl-4-*O*-benzoyl-*myo*-inosityl 1,3,5-orthoformate (3): A solution of pivaloyl chloride (0.390 g, 3.24 mmol) in dry pyridine (3 mL) was added to a stirred, cooled (in an ice bath) solution of *myo*-inosityl 1,3,5-orthoformate (0.570 g, 3.00 mmol) in dry pyridine (5 mL), and the reaction mixture was allowed to reach room temperature. After 12 h, pyridine was evaporated under reduced pressure, the white solid obtained was dissolved in chloroform, washed with water, saturated sodium bicarbonate solution, and brine, and then dried over anhydrous sodium sulfate. The solid obtained from the organic layer on evaporation of the solvent under reduced pressure was crystallized from a mixture of chloroform and petroleum ether to obtain 2-*O*-pivaloyl-*myo*-inosityl 1,3,5-orthoformate (0.520 g, 63 %). mp 159 °C.

Benzoyl chloride (0.240 g, 1.71 mmol) was added to a stirred, cooled solution (in an ice bath) of 2-*O*-pivaloyl-*myo*-inosityl 1,3,5-orthoformate (0.440 g, 1.61 mmol) in dry pyridine (6 mL), and the reaction mixture was allowed to come to room temperature. Stirring was continued for 12 h and pyridine was removed under reduced pressure to obtain a gum, which was worked up with chloroform as above. The unreacted starting material (0.110 g, 25 %) and racemic 2-*O*-pivaloyl-4-*O*-benzoyl-*myo*-inosityl 1,3,5-orthoformate (0.430 g, 71 %) were obtained from the mixture of products by chromatography. M.p 160–161 °C; ^{1}H NMR (200 MHz, $CDCl_3$, 25 °C, TMS): $\delta = 1.28$ (s, 9H), 2.50–2.90 (br s, 1H; D_2O exchangeable), 4.29–4.38 (m, 1H), 4.40–4.49 (m, 1H), 4.54–4.63 (m, 1H), 4.64–4.75 (m, 1H), 5.35–5.43 (m, 1H), 5.60 (d, J(H,H) = 1.5 Hz, 1H), 5.75–5.85 (m, 1H), 7.39–7.53 (m, 2H), 7.54–7.65 (m, 1H), 7.95–8.10 ppm (m, 2H); ^{13}C NMR (50.3 MHz, $CDCl_3$, 25 °C): $\delta = 26.9$, 38.9, 63.0, 67.2, 68.3, 68.5, 69.4, 71.5, 102.8, 128.5, 128.9, 129.8, 133.6, 165.3, 178.5 ppm; IR (Nujol): $\nu = 1706$ (C=O), 1731 (C=O), 3448 cm^{-1} (OH); elemental analysis calcd (%) for $C_{19}H_{22}O_8$ (378.38): C 60.31, H 5.86; found: C 59.93, H 5.69.

Crystals of the 1:1 molecular complex of the orthoformate 1 and the orthoacetate 2 (1·2): The orthoformate **1** (0.200 g, 0.50 mmol) and the orthoacetate **2** (0.200 g, 0.49 mmol) were dissolved in chloroform (3 mL). Petroleum ether (bp 60–80 °C) was diffused into this solution over a period of 7–10 days, to obtain crystals of the 1:1 molecular complex **1·2** (0.300 g, 66 %). M.p. 139–140 °C; ^{1}H NMR (200 MHz, $CDCl_3$, 25 °C, TMS): $\delta = 1.56$ (s, 3H), 2.77–2.82 (d, J(H,H) = 6.0 Hz, 1H; D_2O exchangeable), 2.88–2.92 (d, J(H,H) = 4.0 Hz, 1H; D_2O exchangeable), 5.46–4.53 (m, 2H), 4.53–4.77 (m, 6H), 5.57–5.64 (m, 1H), 5.64–5.71 (m, 2H), 5.72–5.87 (m, 2H), 7.30–7.71 (m, 12H), 7.98–8.23 ppm (m, 8H); IR (Nujol): $\nu = 1706$ (C=O), 1722 (C=O), 3461 cm^{-1} (OH); elemental analysis calcd (%) for $C_{43}H_{38}O_{16}$ (810.76): C 63.70, H 4.72; found: C 63.62, H 4.64.

Solid-state transesterification of *myo*-inosityl orthoesters—general procedure: Crystals of the required *myo*-inositol derivative (0.100 g to 0.500 g) were ground together with sodium carbonate (8 equiv) using a pestle and mortar and the mixture was heated (60 to 168 h) below the melting point of the respective inositol derivative in a hard glass tube under a nitrogen atmosphere. The solid obtained after heating was cooled to ambient temperature, extracted with chloroform followed by methanol; the combined organic extract was evaporated under reduced pressure and the products were separated by column chromatography over silica gel.

Solid-state transesterification of 2: The dibenzoate **2** (0.500 g, 1.25 mmol) and sodium carbonate (1.060 g, 10.0 mmol) were ground together and heated at 140 °C in an atmosphere of nitrogen for 168 h. Isolation of the products as mentioned in the general procedure gave **5**[21] (0.125 g, 19 %), 4,6-di-*O*-benzoyl-*myo*-inosityl 1,3,5-orthoacetate (0.040 g, 8 %), **8**[22] (0.080 g, 21 %), racemic 4-*O*-benzoyl-*myo*-inosityl 1,3,5-orthoacetate[22] (0.060 g, 16 %), and the starting material **2** (0.070 g, 14 %). Data for 4,6-

di-*O*-benzoyl-*myo*-inosityl 1,3,5-orthoacetate: M.p. 160–162 °C; ^{1}H NMR (500 MHz, $CDCl_3$, 25 °C, TMS): $\delta = 1.57$ (s, 3H), 3.15–3.19 (d, J(H,H) = 11.9 Hz, 1H; D_2O exchangeable), 4.20–4.24 (d, J(H,H) = 11.1 Hz, 1H), 4.43–4.46 (m, 2H), 4.84–4.88 (m, 1H), 5.74–5.78 (t, J(H,H) = 4.0 Hz, 2H), 7.15–7.20 (m, 4H), 7.44–7.49 (m, 2H), 7.78–7.81 ppm (dd, J(H,H) = 7.2 Hz, 1.1 Hz, 4H); ^{13}C NMR (50.3 MHz, $CDCl_3$, 25 °C): $\delta = 24.2$, 60.7, 66.8, 68.6, 72.5, 109.7, 128.3, 128.9, 129.8, 133.4, 165.2 ppm; IR ($CHCl_3$): $\nu = 1728$ (C=O), 3186–3569 cm^{-1} (OH); elemental analysis calcd (%) for $C_{22}H_{20}O_8$ (412.40): C 64.08, H 4.89; found: C 64.12, H 5.33.

Solid-state transesterification of 3: The benzoate **3** (0.100 g, 0.26 mmol) and sodium carbonate (0.220 g, 2.08 mmol) were ground together and heated at 140 °C for 168 h. The reaction mixture was worked up as mentioned in the general procedure and **6** (0.018 g, 14%) was isolated by preparative thin-layer chromatography (TLC). M.p. 193–195 °C; ^{1}H NMR (500 MHz, $CDCl_3$, 25 °C, TMS): $\delta = 1.31$ (s, 9H), 4.50–4.53 (m, 2H), 4.92–4.95 (m, 1H), 5.41–5.43 (m, 1H), 5.68–5.70 (d, J(H,H) = 1.2 Hz, 1H), 5.79–5.82 (t, J(H,H) = 3.8 Hz, 2H), 7.16–7.21 (m, 4H), 7.45–7.50 (m, 2H), 7.82–7.86 ppm (dd, J(H,H) = 7.1 Hz, 1.2 Hz, 4H); ^{13}C NMR (75 MHz, $CDCl_3$, 25 °C): $\delta = 27.0$, 39.0, 63.0, 67.0, 68.4, 69.3, 103.3, 128.3, 128.6, 129.8, 133.4, 165.1, 178.2 ppm; IR ($CHCl_3$): $\nu = 1726$ cm^{-1} (C=O); elemental analysis calcd (%) for $C_{26}H_{26}O_9$ (482.49): C 64.72, H 5.43; found: C 64.63, H 5.12. Other products formed in this reaction (eight, as indicated by TLC) were not isolated.

Solid-state transesterification in molecular crystals 1·2: Crystals of the molecular complex **1·2** (0.100 g, 0.12 mmol) and sodium carbonate (0.102 g, 0.96 mmol) were ground together and heated at 120 °C for 168 h. The reaction mixture was worked up as mentioned in the general procedure; a mixture (0.052 g, 41%) of **4** and **5** and a mixture (0.026 g, 35%) of **7** and **8** were isolated by column chromatography over silica gel. Analysis of these mixtures by ^{1}H NMR spectroscopy showed that the tribenzoates **4** and **5** were formed in the ratio 67:33, while the diols **7** and **8** were formed in the ratio 35:65.

Transesterification of 1 in the molten state: Crystals of **1** (0.200 g, 0.50 mmol) were melted in a hard glass tube in an atmosphere of nitrogen at 180 °C and sodium carbonate (0.424 g, 4.00 mmol) was added to this melt and mixed well. The reaction mixture was heated at 180 °C for 36 h. The solid obtained after heating was cooled to ambient temperature, extracted with chloroform followed by methanol; the combined organic extract was evaporated under reduced pressure and the products were separated by preparative thin-layer chromatography to obtain the tribenzoate **4** (0.040 g, 16%), the diol **7** (0.022 g, 15%), 4,6-di-*O*-benzoyl-*myo*-inosityl 1,3,5-orthoformate[22] (0.018 g, 9%), racemic 4-*O*-benzoyl-*myo*-inosityl 1,3,5-orthoformate[22] (0.019 g, 13%), and unreacted **1** (0.045 g, 23%).

Continuation of the reaction for a longer time (50–100 h) resulted in decomposition and charring of the reaction mixture. Transesterification of the diesters **2** and **1·2** in the molten state (as above) also resulted in the formation of a mixture of products; no attempt was made to isolate them.

Transesterification of *myo*-inosityl orthoesters in solution—general procedure: Crystals of the required *myo*-inositol derivative (0.100 g) and dry triethylamine (10 eqûiv) were dissolved in dry acetonitrile (2 mL) and stirred at ambient temperature under a nitrogen atmosphere for 144 h. Acetonitrile and triethylamine were evaporated under reduced pressure and the products were separated by column chromatography over silica gel.

Transesterification of 2: Transesterification as above yielded the tribenzoate **5** (0.038 g, 30%) and the diol **8** (0.022 g, 29%) along with unreacted **2** (0.036 g, 36%).

Transesterification of 3: Transesterification as above yielded the dibenzoate **6** (0.030 g, 23%) and the diol **9** (0.018 g, 25%) along with unreacted **3** (0.046 g, 46%).

Transesterification of 1·2: Transesterification as above yielded a mixture of tribenzoates **4** and **5** (0.041 g, 32%, in the ratio 55:45 as revealed by ^{1}H NMR spectroscopy), a mixture of the diols **7** and **8** (0.021, 28%, in the ratio 56:44 as revealed by ^{1}H NMR spectroscopy) and the starting material (0.030 g, 30%).

Crystal structure analysis: Single crystals of the diesters were obtained from a chloroform/light petroleum mixture and good quality crystals were selected by using a Leica Polarising microscope. X-ray intensity data were collected on a Bruker SMART APEX CCD diffractometer in omega and phi scan modes, $\lambda(Mo_{K\alpha}) = 0.71073$ Å at $T = 293(2)$ K (except for **1**). All the data were corrected for Lorentzian, polarization and absorption effects using Bruker's SAINT and SADABS programs. SHELX-97[23] was used for structure solution and full-matrix least-squares refinement on F^2. Hydrogen atoms were included in the refinement as per the riding model. Crystal data and details of data collection, structure solution, and refinements for **2**, **3**, and **1·2** are summarized in Table 1. All the weak interaction calculations were carried out using PLATON.[24] CCDC-222392–222394 contain the supplementary crystallographic data for this paper. These data can be obtained free of charge from The Cambridge Crystallographic Data Centre via www.ccdc.cam.ac.uk/data_request/cif.

Acknowledgements

We are grateful to the referees for their valuable constructive criticism on our manuscript. We thank Dr. K. M. Sureshan for a sample of the diester **2**. The valuable help by Dr. N. Pawaskar in recording X-ray powder diffractograms and by Dr. S. D. Pradhan in recording the thermograms is gratefully acknowledged. The Department of Science and Technology, New Delhi supported this work. M.P.S. is a recipient of a Senior Research Fellowship of the Council of Scientific and Industrial Research, New Delhi.

[1] a) J. A. Brannigan, G. Dodson, H. J. Duggleby, P. C. E. Moody, J. L. Smith, D. R. Tomchick, A. G. Murzin, *Nature* **1995**, *378*, 416–419; b) D. Voet, J. G Voet, *Mechanisms of Enzyme Action and Metabolism, Biochemistry*, *Vol. 1*, Wiley, New York, **2003**.

[2] S. Patai, *The Chemistry of Functional Groups. The Chemistry of Carboxylic Acids and Esters*, (Ed.: S. Patai), Wiley, New York, **1969**, p. 1155.

[3] T. Praveen, U. Samanta, T. Das, M. S. Shashidhar, P. Charkrabarti, *J. Am. Chem. Soc.* **1998**, *120*, 3842–3845.

[4] a) Y. Ohashi, K. Yanagi, T. Kurihara, Y. Sasada, Y. Ohgo, *J. Am. Chem. Soc.* **1982**, *104*, 6353–6359; b) J. H. Kim, S. M. Hubig, S. V. Lindeman, J. K. Kochi, *J. Am. Chem. Soc.* **2001**, *123*, 87–95; c) M. A. Garcia-Garibay, *Acc. Chem. Res.* **2003**, *36*, 491–498; d) K. Tanaka, F. Toda, *Chem. Rev.* **2000**, *100*, 1025–1074; e) D. Braga, F. Grepioni, *Angew. Chem.* **2004**, *116*, 4092–4102; *Angew. Chem. Int. Ed.* **2004**, *43*, 4002–4011.

[5] a) C. N. Sukenik, J. A. P. Bonapace, N. S. Mandel, P.-Y. Lau, G. Wood, R. G. Bergman, *J. Am. Chem. Soc.* **1977**, *99*, 851–858; b) C. P. Tang, H. C. Chang, R. Popovitz-Biro, F. Frolow, M. Lahav, L. Leiserowitz, R. K. McMullan, *J. Am. Chem. Soc.* **1985**, *107*, 4058–4070; c) W. Jones, J. M. Thomas, *Proc. Indian Natl. Sci. Acad. Part A* **1986**, *52*, 363–378; d) H. C. Chang, R. Popovitz-Biro, M. Lahav, L. Leiserowitz, *J. Am. Chem. Soc.* **1987**, *109*, 3883–3893; e) Y. Weisinger-Lewin, M. Vaida, R. Popovitz-Biro, H. C. Chang, F. Manning, F. Frolow, M. Lahav, L. Leiserowitz, *Tetrahedron* **1987**, *43*, 1449–1475; f) J. A. R. P. Sarma, J. D. Duntiz, *Acta Crystallogr. Sect. B* **1990**, *46*, 780–784; g) K. Vyas, H. Manohar, K. Venkatesan, *J. Phys. Chem.* **1990**, *94*, 6069–6073; h) V. Enkelmann, G. Wegner, K. Novak, K. B. Wagener, *J. Am. Chem. Soc.* **1993**, *115*, 10390–10391; i) J. D. Dunitz, *Acta Crystallogr. Sect. B* **1995**, *51*, 619–631; j) M. Kaftory in *Organic Solid State Reaction*, (Ed.: F. Toda), Kluwer Academic Publishers, Dordrecht, **2002**, pp. 47–67.

[6] a) V. Ramamurthy, K. Venkatesan, *Chem. Rev.* **1987**, *87*, 433–481; b) K. Honda, F. Nakanishi, N. Feeder, *J. Am. Chem. Soc.* **1999**, *121*, 8246–8250; c) T. Obata, T. Shimo, M. Yasutake, T. Shinmyozu, M. Kawaminami, R. Yoshida, K. Somekawa, *Tetrahedron* **2001**, *57*,

1531–1541; d) T. Hasegawa, K. Ikeda, Y. Yamazaki, *J. Chem. Soc. Perkin Trans. 1* **2001**, 3025–3028.

[7] a) In our on-going programme on the synthesis of biologically relevant *myo*-inositol derivatives,[7b] we developed the racemic dibenzoate **1** as a versatile intermediate for the preparation of several protected *myo*-inositol derivatives.[7c,d] During this work we observed that the preparations of the racemic dibenzoate **1** (on several gram scale) was always contaminated with the tribenzoate **4** as well as the diol **7** and required several crystallizations or column chromatographic separation to get rid of the contaminating benzoates **4** and **7**. Careful observations during the preparation of the dibenzoate **1** indicated that the amount of contamination increased on storage (either in solution or as a precipitate in the mother liquor or as a crude solid) with the presence of bases. Further systematic experimentation showed that the dibenzoate **1** underwent transesterification with extreme ease in many organic solvents, in the presence of weak bases such as pyridine and solid sodium carbonate. We then wondered whether a solvent was necessary at all for the transesterification of **1** and conducted experiments in the solid-state which are published;[3] b) K. M. Sureshan, M. S. Shashidhar, T. Praveen, T. Das, *Chem. Rev.* **2003**, *103*, 4477–4504; c) T. Das, T. Praveen, M. S. Shashidhar, *Carbohydr. Res.* **1998**, *313*, 55–59; d) T. Das, M. S. Shashidhar, *Carbohydr. Res.* **1998**, *308*, 165–168.

[8] Helical organization through hydrogen bonding has extensively been studied in phenols; see a) P. I. Coupar, C. Glidewell, G. Fergusson, *Acta Crystallogr. Sect. B:* **1997**, *53*, 521–533; b) E. S. Lavender, G. Ferguson, C. Glidewell, *Acta Crystallogr. Sect. C* **1999**, *55*, 430–432.

[9] a) A. Matsumoto, T. Tanaka, T. Tsubouchi, K. Tashiro, S. Saragai, S. Nakamoto, *J. Am. Chem. Soc.* **2002**, *124*, 8891–8902; b) A. Matsumoto, K. Sada, K. Tashiro, M. Miyata, T. Tsubouchi, T. Tanaka, T. Odani, S. Nagahama, T. Tanaka, K. Inoue, S. Saragai, S. Nakamoto, *Angew. Chem.* **2002**, *114*, 2612–2615; *Angew. Chem. Int. Ed.* **2002**, *41*, 2502–2505; c) S. Nagahama, K. Inoue, K. Sada, M. Miyata, A. Matsumoto, *Cryst. Growth Des.* **2003**, *3*, 247–256; d) D. Fujimoto, R. Tamura, Z. Lepp, H. Takashashi, T. Ushio, *Cryst. Growth Des.* **2003**, *3*, 973–979.

[10] T. Banerjee, M. S. Shashidhar, *Tetrahedron Lett.* **1994**, *35*, 8053–8056.

[11] a) H. B. Bürgi in *Perspectives in Coordination Chemistry* (Eds.: A. F. Williams, C. Floriani, A. E. Mercbach), VCH, Weinheim, **1993**, pp. 1–29; b) H. B. Bürgi, J. D. Dunitz in *Structure Correlation*, *Vol. 2* (Eds.: H. B. Bürgi, J. D. Duntiz), VCH, Weinheim, **1994**, pp. 767–784.

[12] a) H. B. Bürgi, J. D. Dunitz, E. Shefter, *J. Am. Chem. Soc.* **1973**, *95*, 5065–5067; b) H. B. Bürgi, J. D. Dunitz, E. Shefter, *Acta Crystallogr. Sect. B* **1974**, *30*, 1517–1527; c) H. B. Bürgi, J.-M. Lehn, G. J. Wipff, *J. Am. Chem. Soc.* **1974**, *96*, 1956–1957; d) H. B. Bürgi, J. D. Dunitz, *Acc. Chem. Res.* **1983**, *16*, 153–161.

[13] a) M. Marquart, J. Walter, J. Deisenhofer, W. Bode, R. Huber, *Acta Crystallogr. Sect. B* **1983**, *39*, 480–490; b) P. Chakrabarti, D. Pal, *Protein Sci.* **1997**, *6*, 851–859.

[14] a) M. Nishio, M. Hirota, Y. Umezawa, *The CH/π Interaction: Evidence, Nature and Consequences*, Wiley-VCH, Weinheim, **1998**; b) M. Yamakawa, I. Yamada, R. Noyori, *Angew. Chem.* **2001**, *113*, 2900–2903; *Angew. Chem. Int. Ed.* **2001**, *40*, 2818–2821; c) M. Nishio, *CrystEngComm* **2004**, *6*, 130–158; d) R. Boese, T. Clark, A. Gavezzotti, *Helv. Chim. Acta* **2003**, *86*, 1085–1100.

[15] G. R. Desiraju, T. Steiner, *The Weak Hydrogen Bond in Structural Chemistry and Biology*, Oxford University Press, New York, **1999**.

[16] T. C. Bruice, *Acc. Chem. Res.* **2002**, *35*, 139–148.

[17] C. D. Tatko, M. L. Waters, *J. Am. Chem. Soc.* **2004**, *126*, 2028–2034.

[18] M. Brandl, M. S. Weiss, A. Jabs, J. Suhnel, R. Hilgenfeld, *J. Mol. Biol.* **2001**, *307*, 357–377.

[19] a) Y. Umezawa, S. Tsuboyama, K. Honda, J. Uzawa, M. Nishio, *Bull. Chem. Soc. Jpn.* **1998**, *71*, 1207–1213; b) Y. Umezawa, S. Tsuboyama, H. Takahashi, J. Uzawa, M. Nishio, *Tetrahedron* **1999**, *55*, 10047–10056; Also see d) E. J. Corey, J. J. Rhode, A. Fischer, M. D. Azimioara, *Tetrahedron Lett.* **1997**, *38*, 33–36; e) E. J. Corey, J. J. Rohde, *Tetrahedron Lett.* **1997**, *38*, 37–40; f) I. Washington, K. N. Houk, *Angew. Chem.* **2001**, *113*, 4617–4620; *Angew. Chem. Int. Ed.* **2001**, *40*, 4485–4488.

[20] a) V. R. Thalladi, T. Smolka, A. Gehrke, R. Boese, R. Sustmann, *New J. Chem.* **2000**, *24*, 143–147; b) R. Boese, M. T. Kirchner, W. E. Billups, L. R. Norman, *Angew. Chem.* **2003**, *115*, 2005–2007; *Angew. Chem. Int. Ed.* **2003**, *42*, 1961–1963; c) J. Zyss, I. Ledoux-Rak, H-C. Weiss, D. Bläeser, R. Boese, P. K. Thallapally, V. R. Thalladi, G. R. Desiraju, *Chem. Mater.* **2003**, *15*, 3063–3073.

[21] T. Praveen, M. S. Shashidhar, *Carbohydr. Res.* **2001**, *330*, 409–411.

[22] K. M. Sureshan, M. S. Shashidhar, *Tetrahedron Lett.* **2000**, *41*, 4185–4188.

[23] G. M. Sheldrick, SHELX97, Program for crystal structure solution and refinement, University of Göttingen (Germany) **1997**.

[24] A. L. Spek, PLATON, Bijvoet Center for Biomedical Research, Vakgroep Kristal-en Structuuchemie, University of Utrecht (The Netherlands) **1990**.

Received: August 17, 2004
Published online: February 15, 2005